

Feasibility of “natural surface” epicardial mapping from the pulmonary artery for management of atrial arrhythmias



Jeffrey J. Smietana, MD,¹ Fermin C. Garcia, MD, FHRS,¹
Naga Venkata K. Pothineni, MD,¹ Kelvin Bush, MD, Mirmilad Khoshknab, MD,
Timothy M. Markman, MD, Pasquale Santangeli, MD, PhD, FHRS, Sanjay Dixit, MD, FHRS,
Frank Marchlinski, MD, FHRS, Cory Tschabrunn, PhD, Saman Nazarian, MD, PhD, FHRS

From the Electrophysiology Section, Division of Cardiovascular Medicine, Hospital of the University of Pennsylvania, Philadelphia, Pennsylvania.

BACKGROUND The right and left pulmonary artery branches (RPA, LPA) overlie inaccessible left atrial (LA) epicardium, containing the Bachmann bundle (BB), that participate in arrhythmia pathogenesis and offer an opportunity for natural surface epicardial mapping (NSEM).

OBJECTIVE We sought to assess the feasibility of NSEM of BB and LA roof arrhythmias.

METHODS Electrogram recording, pacing, and ablation was performed in 2 swine. Subsequently, NSEM and pacing from the RPA and LPA was performed in 11 consecutive patients undergoing ablation of atrial fibrillation or flutter. Pacing entrainment and ablation of LA epicardium, from the pulmonary artery (PA), was performed in cases of atypical flutter.

RESULTS Swine specimens revealed no vascular disruption and LA epicardial lesions up to 7 mm in diameter and 3 mm in depth. In clinical cases, RPA mapping was performed in 11 (100%) and LPA mapping in 6 (55%) patients. Simultaneous leftward activation of the BB followed by rightward activation of the opposing LA endo-

cardium was recorded during crista pacing. Right and left PA median signal amplitudes were 0.71 mV and 0.30 mV, respectively. Endocardial LA median distance was 9 mm to the RPA and 15.6 mm to the LPA and LA capture was successful in 7 of 8 (88%). In cases of atypical flutter, entrainment was successful in 3 of 3 (100%) and ablation was performed.

CONCLUSION PA NSEM can enable safe recording and entrainment of the BB, providing otherwise inaccessible epicardial arrhythmia measurements. The safety and efficacy of ablation from the PA requires further study.

KEYWORDS Atrial flutter; Atrial fibrillation; Pulmonary artery; Bachmann bundle; Catheter ablation; Epicardial mapping; Epicardial ablation

(Heart Rhythm 0² 2021;2:578–587) © 2021 Heart Rhythm Society. Published by Elsevier Inc. This is an open access article under the CC BY-NC-ND license (<http://creativecommons.org/licenses/by-nc-nd/4.0/>).

Introduction

The Bachmann bundle (BB)¹ describes a parallel set of epicardial fibers along the interatrial groove with bifurcating extensions into atrial endocardial myocardium. The BB extends from the right atrium at the distal end of the anterior internodal pathway,² the superior vena cava (SVC), and the right atrial (RA) appendage, toward the left atrium (LA) surrounding the left atrial appendage (LAA) and the left lateral ridge.³ Fiber orientation disarray and de novo or ablation-induced fibrosis of BB muscle fibers may predispose to interatrial conduction delay and/or development of atrial arrhythmia.^{4,5} There is clinical evidence for the participation

of epicardial fibers such as the BB in the pathogenesis of atrial arrhythmias.^{6–8} However, endocardial mapping and ablation of putative epicardial arrhythmia circuitry is limited by intervening endocardial myocardium, fibrosis, and/or fatty tissues. Percutaneous epicardial mapping of the LA from the oblique sinus has offered insight into atrial arrhythmia mechanisms and provide adjunctive treatment strategies for atrial fibrillation (AF) and atypical atrial flutter (AFL).^{9–12} However, this approach is limited by pericardial reflections, which restrict access to the roof and superior pulmonary veins (PV) where critical epicardial structures, BB and the ligament of Marshall, are positioned.^{13,14} In addition, percutaneous epicardial mapping comes with added procedural risk.¹⁵ “Natural orifice” surgical or endoscopic approaches have been explored by other fields for improved anatomic access to sites of interest.^{16,17} Based on image fusion and intracardiac echocardiography

¹The first 3 authors contributed equally to the study. **Address reprint requests and correspondence:** Dr Saman Nazarian, Hospital of the University of Pennsylvania, 3400 Spruce St, Cardiac EP, Founders 9118, Philadelphia, PA 19104. E-mail address: Saman.Nazarian@pennmedicine.upenn.edu.

KEY FINDINGS

- Natural surface epicardial mapping from the right and left main pulmonary artery is a means for electrogram recording of the Bachmann bundle and epicardial roof muscle fibers.
- Epicardial signals from the pulmonary artery can be safely recorded and in select cases of atypical flutter, the arrhythmia can be successfully entrained from this location.
- Pulmonary artery recordings provide arrhythmia characteristics that may not be otherwise visible on the left atrial endocardial surface and may guide anatomical endocardial ablation.
- Anatomic variability exists in distance from the pulmonary artery to the epicardial left atrium, and myocardial capture threshold may be a surrogate for proximity and an index of direct continuity.
- The safety and efficacy of an adjunctive strategy of ablation from the pulmonary artery requires further study.

(ICE), we have observed that the left and right pulmonary arteries (PA) overlie these inaccessible epicardial roof structures and offer an opportunity for “natural surface” epicardial mapping (NSEM).

Objective

In this study we sought to test the hypothesis that NSEM from the right and left main PA provides (1) methodology for electrogram recording of the BB and epicardial roof muscle fibers, as well as (2) methodology for interaction with epicardial roof arrhythmia circuitry using entrainment and ablation (Figure 1).

Methods

Animal experiments

Given a similar anatomic relationship between the PA and the LA, the feasibility of mapping and ablation from the PA was evaluated in 2 swine. The research protocol was approved by the Institutional Animal Care and Use Committee of the University of Pennsylvania and conformed to the position of the American Heart Association on Research Animal Use. All experiments were performed at the University of Pennsylvania Translational Cardiac Electrophysiology Laboratory in Philadelphia, PA. Mapping was performed with a 3.5 mm catheter and an electroanatomic mapping system (ThermoCool SmartTouch SF and CARTO 3; Biosense Webster, Diamond Bar, CA). Irrigated lesions were delivered to the PA adjacent to the opposing endocardium at 30 W for 30 seconds. Following the experiments, the animals were sacrificed, and the integrity of the PA and LA and extent of lesions were assessed by gross examination.

Clinical studies

The Institutional Review Board of the Hospital of the University of Pennsylvania approved our prospective Atrial Fibrillation Registry Cohort. All patients gave informed consent for the use of clinical, imaging, and procedural data for medical research prior to the procedure. Data from 11 consecutive patients with an indication for catheter ablation of AF or atypical AFL according to the 2014 AHA/ACC/HRS guidelines for the management of patients with atrial fibrillation¹⁸ undergoing the procedure at the Hospital of the University of Pennsylvania were included in the study. The procedures were performed using general anesthesia with high-frequency, low-volume ventilation. Anticoagulation was not interrupted for the procedures. ICE was used to guide transseptal puncture, monitor for procedural complications, and facilitate mapping and ablation. Decapolar diagnostic catheters were placed in the proximal coronary sinus (CS) and along the crista terminalis. Dual or single transseptal punctures were performed based upon operator preference. Multipolar mapping (PentaRay, Biosense Webster, Diamond Bar, CA; or HD Grid, Abbott, Chicago, IL) and contact force-sensing open-irrigated ablation catheters (ThermoCool, Biosense Webster, Diamond Bar, CA; or TactiCath, Abbott, Minneapolis, MN) were utilized. Electroanatomic mapping was performed using CARTO 3 (Biosense Webster, Diamond Bar, CA) in 10 patients (91%) and EnSite Velocity (Abbott, Chicago, IL) in 1 patient (9%). Bipolar signals were notch filtered at 60 Hz and bandpass filtered at 16–500 Hz and 30–300 Hz, respectively. The mapping catheter alone can be directly navigated into the PA, but for the majority of cases, PA mapping was performed with the aid of a steerable sheath. The ablation catheter was advanced into the right ventricular outflow tract under fluoroscopic and ICE guidance, taking care to avoid force >5 gm, to avoid mechanical complications. The steerable sheath was then railed over the catheter using the deflection to negotiate the upward and rightward turn from the main PA into the right main PA (Figure 2). The ablation catheter could then be used for PA mapping or exchanged for a multipolar catheter to record LA epicardial signals. Pacing from the PA with up to 50 mA at 2.0 ms was performed to assess for LA capture. Entrainment from the PA was performed during cases of atrial flutter. In cases with favorable entrainment characteristics radiofrequency ablation was applied at low power (<30 watts) for up to 30 seconds per lesion. The left main coronary artery position, well below the main PA branches and at the level of the posterior right ventricular outflow tract, was confirmed on ICE prior to ablation. Continuous variables are reported as mean and standard deviation or median and interquartile range (IQR) as appropriate; categorical variables are reported as proportions or percentages.

Results

In vivo animal studies

The PA-to-LA anatomy relationship in the swine was similar to that of human anatomy. Capture of LA myocardium from

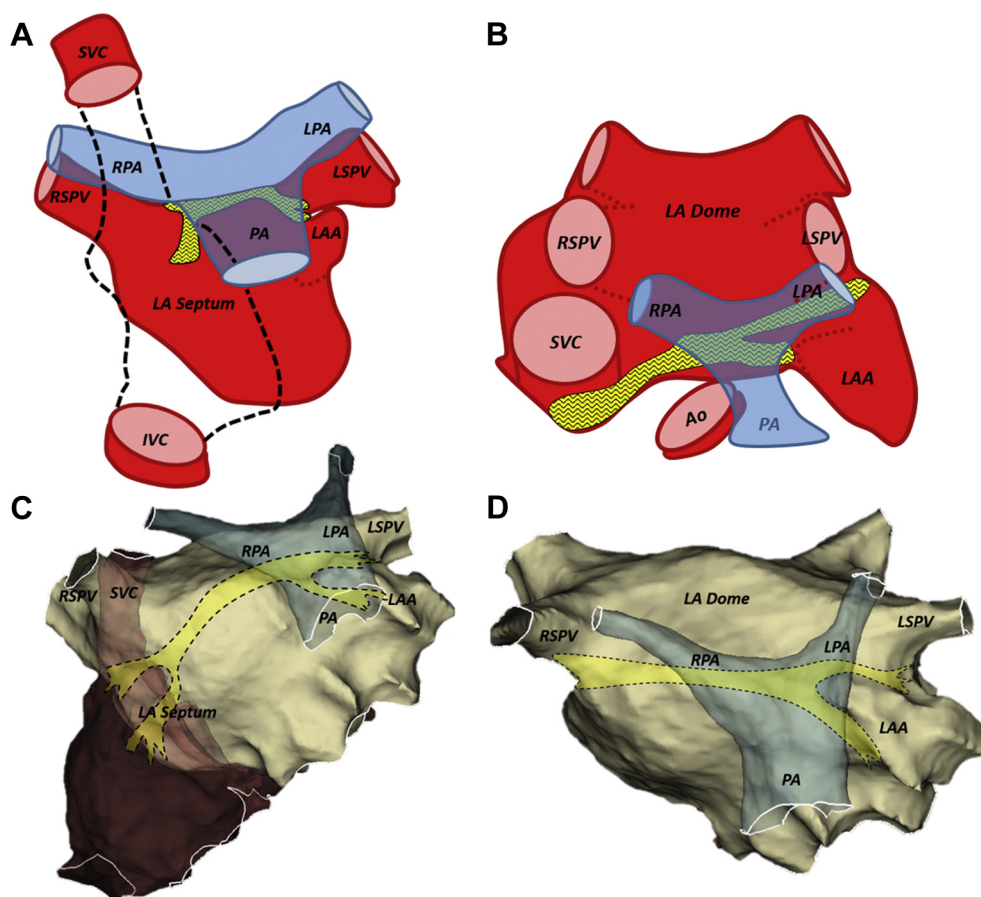


Figure 1 A, B: A graphical representation showing the relationship of the left atrium (red) with the left and right pulmonary artery (blue) and Bachmann bundle (BB) (yellow); C, D: corresponding anatomical map (EnSite Velocity; Abbott, Chicago, IL). A, C: The left atrium as viewed from the left atrial (LA) septum with the right atrium transparent (dotted line) and the anatomical course of the BB. C, D: The left atrium as viewed above from the LA dome and the anatomical course of BB. Ao = aorta; IVC = inferior vena cava; LA = left atrium; LAA = left atrial appendage; LPA = left pulmonary artery; LSPV = left superior pulmonary vein; PA = pulmonary artery; RPA = right pulmonary artery; RSPV = right superior pulmonary vein; SVC = superior vena cava.

the PA was possible in both animal studies at 15 mA at 2.0 ms. Ten lesions, 5 per animal, were delivered using irrigated radiofrequency at 30 W for 30 seconds within the PA opposing the LA. Upon gross examination, a series of these lesions extended from the PA to the LA epicardium up to 7 mm in diameter and up to 3 mm in depth (Figure 3). No endocardial dissection or disruption of the PA was noted using these power and duration settings.

Clinical studies

A total of 11 consecutive patients (91% male) with mean age of 69 ± 9.7 years underwent elective catheter ablation of AF (6, 55%) or atypical AFL (5, 45%). Six (55%) had previously undergone a prior AF ablation. Baseline patient characteristics are reported in Table 1. Access to the PA and right and left main branches directly overlying the LA roof was possible in all patients and recoding from the right and/or left PA was at the discretion of the primary operator. There were no procedural complications. Electrogram recording in the PA was performed using a multipolar catheter (8, 73%) and/or an ablation catheter (3, 27%). The right main PA was mapped in 11 (100%) and the left main PA

was mapped in 6 (55%). The mapped rhythm was sinus (3, 27%), atrial paced (4, 36%), or LA flutter (4, 36%) (Table 2).

PA signal electrograms

Atrial signal recording from the right PA yielded a median amplitude of 0.71 mV (IQR 0.36–0.77 mV) and an adjacent endocardial LA roof median amplitude of 1.61 mV (IQR 0.36–4.0 mV). The signal amplitude from the left PA had a median measurement of 0.30 mV (IQR 0.23–0.47 mV) and an adjacent endocardial LA ridge median amplitude of 1.67 mV (range 0.65–3.07 mV). Distance measurement between endovascular and endocardial boundaries on the electroanatomic map revealed right main PA median distance of 9 mm (IQR 7.15–10.28) and left main PA median distance of 15.6 mm (range 10.3–19.6 mm) to the closest LA endocardial point (Table 3).

PA pacing

Pacing from the PA was performed in 8 (73%) patients at both standard (10 mA at 2.0 ms) and high outputs (50 mA at 2.0 ms). Successful LA capture was observed in 7 (88%)

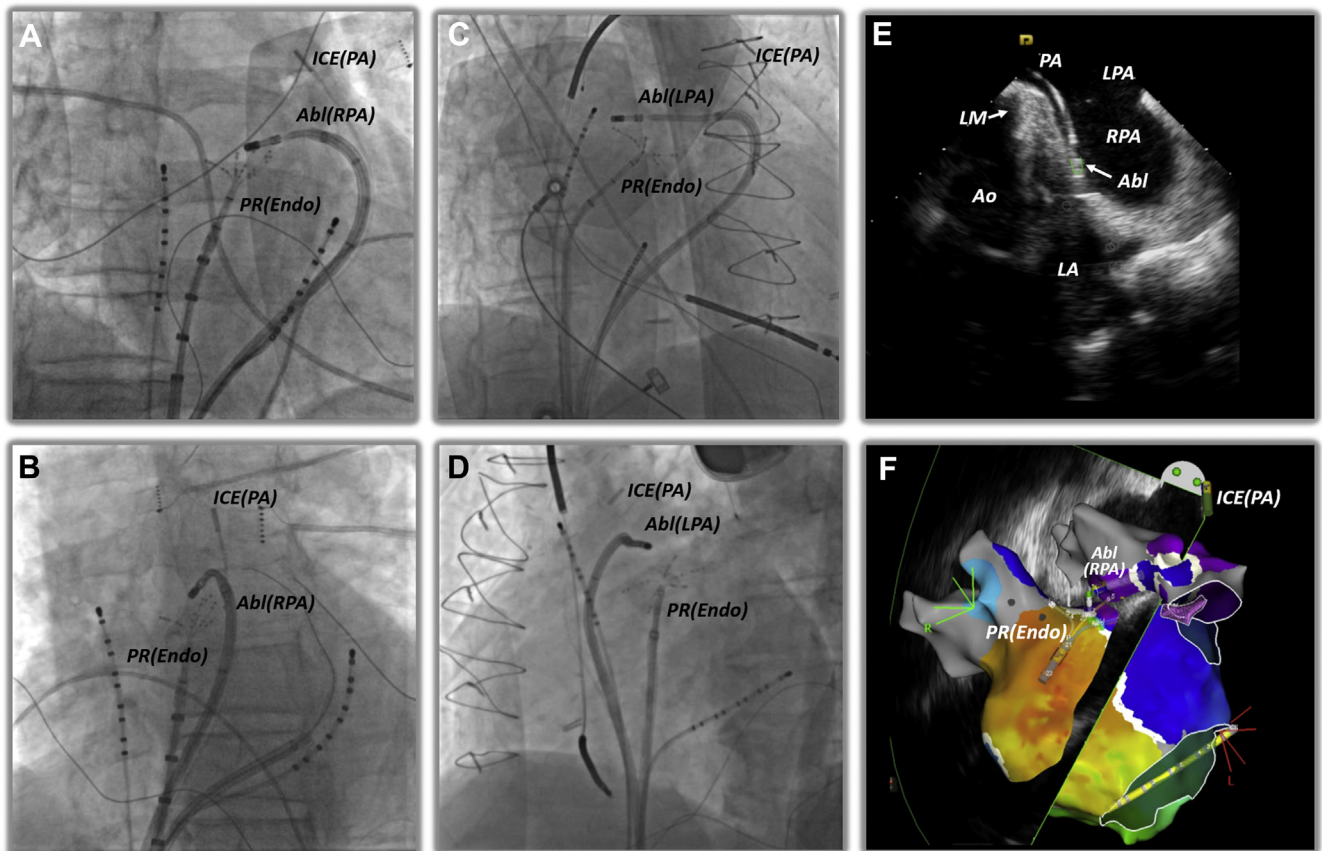


Figure 2 Fluoroscopic and intracardiac echocardiographic position of the ablation and mapping catheters. **A:** Right anterior oblique (RAO) and **B:** left anterior oblique (LAO) projection of an ablation catheter in the right pulmonary artery (PA). **C:** RAO and **D:** LAO projection of an ablation catheter in the left PA. **E:** Intracardiac echocardiography (ICE) catheter from the PA demonstrating the main PA bifurcation and an ablation catheter in the right PA. **F:** Electroanatomic map of the left atrium and PA shown with respect to the ICE image from panel E. Abl = ablation catheter; Ao = aorta; Endo = endocardium; LPA = left pulmonary artery; LM = left main; PR = PentaRay; RPA = right pulmonary artery.

patients. One (13%) captured at 10 mA from the right PA, 5 (63%) captured at 50 mA from the right PA, 1 (13%) captured at 50 mA from the left PA, and 1 (13%) was unable to capture despite maximum output pacing (Table 3). CS activation patterns were recorded in patients in whom successful PA capture occurred during underlying sinus rhythm. This consisted of 4 patients, all with capture from the right PA. The activation of the CS was proximal-to-distal in 2 patients and distal-to-proximal in the remaining 2 patients. The pattern of activation was not influenced by prior mitral annular or cavotricuspid isthmus ablation.

Bachmann bundle mapping

In 3 patients, presenting for an index catheter ablation of paroxysmal AF, indirect mapping of BB from the PA was performed to demonstrate feasibility of true epicardial mapping distinct from LA endocardial activation. The proximal crista catheter was paced while activation mapping of the LA and right main PA was performed. In 2 patients, the activation map revealed earliest epicardial activation over the PA, an indirect recording of BB, with the activation wavefront moving away from the septum. The LA endocardial activation followed the epicardial activation recorded from the PA, showing a

broad breakthrough wavefront moving in the opposing direction toward the septum. Although BB has previously been recorded from the PA as early as 1978,^{19,20} to our knowledge these are the first in vivo human recordings demonstrating BB activation with competing epicardial and endocardial wavefronts of RA-to-LA activation, supporting a bilayer activation pattern in the LA roof (Figure 4 and Supplemental Video 1). In the third patient, earliest RA-to-LA activation occurred at the interatrial septum, suggesting diseased BB conduction. The P-wave duration averaged over 12 leads in this patient during atrial pacing was 168 ms, compared to 126.5 ± 9.2 ms among the patients with earliest BB conduction to the LA roof. Similarly, the interauricular activation time as measured from the RA catheter positioned at the crista terminalis to the distal CS catheter, in the patient with earliest LA activation in the septum, was 185 ms vs 139 ± 19.8 ms among the patients with earliest BB conduction to the LA roof.

Atypical atrial flutter

In the patients with atypical AFL (5, 45%), entrainment and ablation from the PA was attempted in 3. Further case details of these patients are presented to highlight the potential utility of this novel approach.

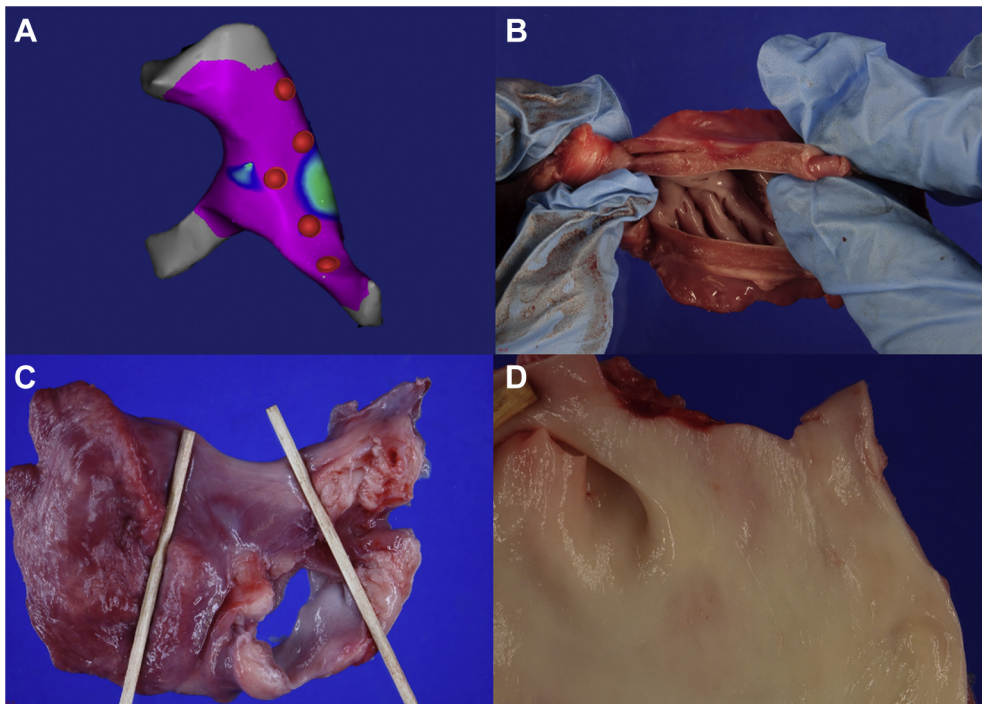


Figure 3 Lesions delivered from the pulmonary artery (PA) to the left atrium (LA) roof in swine animal model. **A:** Electroanatomic mapping of the PA and locations of irrigated radiofrequency lesion delivery (30 W × 30 seconds each). **B:** Illustration of the depth of a lesion in a transverse cut through the PA and LA roof with the lesion reaching the epicardial LA. **C:** The epicardial LA roof lesion with the PA surgically removed. **D:** The endovascular PA lesion without any evidence of dissection or vascular disruption.

Atypical AFL patient 1

A 67-year-old man who had previously undergone multiple prior ablations with a pulmonary vein isolation (PVI), posterior wall isolation, anterior mitral line (AML), and cavotricuspid isthmus line presented with recurrence of atypical AFL with a cycle length (CL) of 300 ms and proximal-to-distal CS activation. Entrainment revealed postpacing interval exceeding tachycardia cycle length (PPI-TCL) by <30 ms along the mitral annulus, LA roof, and RA septum, but >30 ms from lateral right atrium and crista terminalis. Right PA mapping was performed in the anatomical location of BB, which revealed continuous activation signals (Figure 5A). Successful capture and entrainment from the right PA was performed at 50 mA at 2.0 ms with PPI-TCL of 12 ms (Figure 5B). Ablation lesions were delivered from the PA at 30 watts for 20–30 seconds, which resulted in tachycardia slowing to a CL of 320 ms. Ablation was then performed from the adjacent endocardium despite only a small far-field signal (0.25 mV), which resulted in termination of the tachycardia (Figure 5C). AML bidirectional block was confirmed, and the case was concluded.

Atypical AFL patient 2

A 64-year-old man who had previously undergone PVI presented with atypical AFL. Entrainment was consistent with mitral annular flutter utilizing the LA ridge at a CL of 260 ms with a proximal-to-distal activation sequence. An

Table 1 Baseline clinical characteristics

Demographics	Result
Male sex	10/11 (91%)
Mean age	69 ± 9.6
Mean BMI (kg/m ²)	27.6 ± 3.7
Past medical history	
Hypertension	6/11
Diabetes	2/11
Coronary artery disease	5/11
Cerebrovascular event	1/11
Mean CHADSVASc	2.4 ± 1.9
Atrial fibrillation procedural history	
Prior catheter ablation	6/11 (45%)
Prior pulmonary vein isolation	6/6 (100%)
Prior posterior wall isolation	4/6 (67%)
Prior mitral line	2/6 (33%)
Prior CTI line	2/6 (33%)
Other ablation	2/6 (33%)
Transthoracic echocardiography	
Mean LVEF (%)	51.6 ± 15.7
Mean left atrial size (cm)	4.4 ± 0.7
Medications	
Novel oral anticoagulant	10/11 (91%)
Vitamin K antagonist	1/11 (9%)
Beta blocker	10/11 (91%)
Amiodarone	1/11 (9%)
Dofetilide	1/11 (9%)
Sotalol	1/11 (9%)

Data shown as number of patients (n/total) and percentage (%), or mean ± standard deviation.

BMI = body mass index; CTI = cavotricuspid isthmus.

Table 2 Procedural details

Detail	n/total (%)
Procedure indication	
Atrial fibrillation	6/11 (55%)
Atypical atrial flutter	5/11 (45%)
Pulmonary artery mapping	
Right PA mapping	11/11 (100%)
Left PA mapping	6/11 (55%)
Mapped rhythm	
Sinus rhythm	3/11 (27%)
Atrial paced rhythm	4/11 (36%)
Atypical atrial flutter	4/11 (36%)
Mapping system	
CARTO 3D	10/11 (91%)
EnSite Velocity	1/11 (9%)
Pulmonary artery mapping catheter	
Ablation catheter	8/11 (73%)
Multipolar catheter	3/11 (27%)

Data shown as number of patients (n/total).
PA = pulmonary artery.

AML was performed with tachycardia slowing to 310 ms but with failure to terminate the tachycardia. A portion of the AML that traversed the septum was reinforced from the opposing right atrium. A line was then drawn from the anterior mitral line to the top of the LAA, where continued slowing occurred. Entrainment revealed PPI-TCL <30 ms on the LA ridge and ablation in this region was targeted extensively from the PV and LAA sides, with further slowing to 340 ms. Further attempts at targeting this area with ethanol were considered, but CS venography revealed no vein of Marshall (VOM). PA mapping was then performed. Entrainment was attempted from the right PA without capture. Ablation lesions were delivered from the PA at 30 W for 20 seconds opposing the AML to reinforce the endocardial lesion set, with no effect. Successful entrainment was then performed from the left main PA at 50 mA at 2.0 ms with a PPI-TCL of 17 ms (Figure 5D). Ablation was performed in the left PA at 20 W for 20 seconds in areas with a short return cycle following entrainment (<20 ms), with no effect on the arrhythmia. The patient was cardioverted and bidirectional endocardial block was confirmed across the AML. The left PVs were reisolated and the procedure was concluded without achieving termination of the tachycardia during ablation.

Atypical AFL patient 3

A 60-year-old man who had previously undergone 2 prior catheter ablations including PVI, posterior wall isolation, a lateral mitral line, and scar modification presented with atypical AFL. Entrainment was consistent with a biatrial flutter at 290 ms with distal-to-proximal CS activation. Entrainment revealed PPI-TCL <30 ms along the mitral annulus, LA roof, and RA septum, and >30 ms on the posterior wall. Entrainment from the right PA was achieved at 10 mA at 2.0 ms and revealed PPI-TCL of 20 ms. Ablation lesions were delivered from the PA at 30 W for up to 30 seconds, with no effect on the tachycardia, but the PW that had

Table 3 Pulmonary artery characteristics

Characteristic	Result
Pulmonary artery pacing	
Successful capture	7/8 (88%)
Right PA at 50 mA	5/8 (63%)
Right PA at 10 mA	1/8 (13%)
Left PA at 50 mA	1/8 (13%)
Left PA at 10 mA	0/8 (0%)
Pulmonary artery signal recording	
Right PA (mV)	0.71 (0.36–0.77)
Left PA (mV)	0.3 (0.23–0.47)
Adjacent endocardial signal recording	
Endocardial LA roof (mV)	1.61 (0.36–4.0)
Endocardial LA ridge (mV)	1.67 (0.65–3.07)
Pulmonary artery to endocardial LA distance	
Right PA distance (mm)	9.1 (7.15–10.28)
Left PA distance (mm)	15.6 (10.3–19.6)
Mean baseline impedance (ohm)	
Patient #1	135 ± 5
Patient #2	138 ± 10
Patient #3	133 ± 2
Mean impedance drop (ohm)	
Patient #1	11 ± 4
Patient #2	15 ± 2
Patient #3	6 ± 1

Data shown as number of patients (n/total) and percentage (%), median with interquartile range, or mean ± standard deviation.

LA = left atrium; PA = pulmonary artery.

reconnected was now isolated, suggesting an epicardial connection to the PW, likely the septopulmonary bundle that was targeted at the LA roof. Adjacent endocardial ablation on the LA roof slowed the tachycardia (415 ms). The tachycardia terminated with a lateral mitral line and block across the lateral line was achieved with ethanol ablation of the VOM.

Discussion

Catheter ablation is now standard of care for the management of AF and AFL.¹⁸ Creation of conduction block is the cornerstone of catheter ablation. Despite significant technological advances in ablation platforms, arrhythmia recurrences are frequently encountered. Recovery of conduction across prior endocardial ablation lines and inability to achieve transmural lesions are important etiologies for arrhythmia recurrences requiring repeat procedures.²¹

The epicardium of the LA is recognized as a critical component of arrhythmogenesis, often harboring fixed macroreentrant circuits that are challenging to ablate from the endocardium. The BB and other epicardial fibers potentially also contribute to functional reentry, AF initiation, and maintenance.^{22,23} Despite years of open or thoracoscopic surgical AF ablation, the experience has been primarily anatomical and limited by the lack of high-density mapping of arrhythmia circuits. Percutaneous epicardial approaches for AF/AFL ablation have evolved with improved understanding of the role of the LA epicardium.²⁴ Studies have revealed regions of preserved epicardial conduction across the PV and

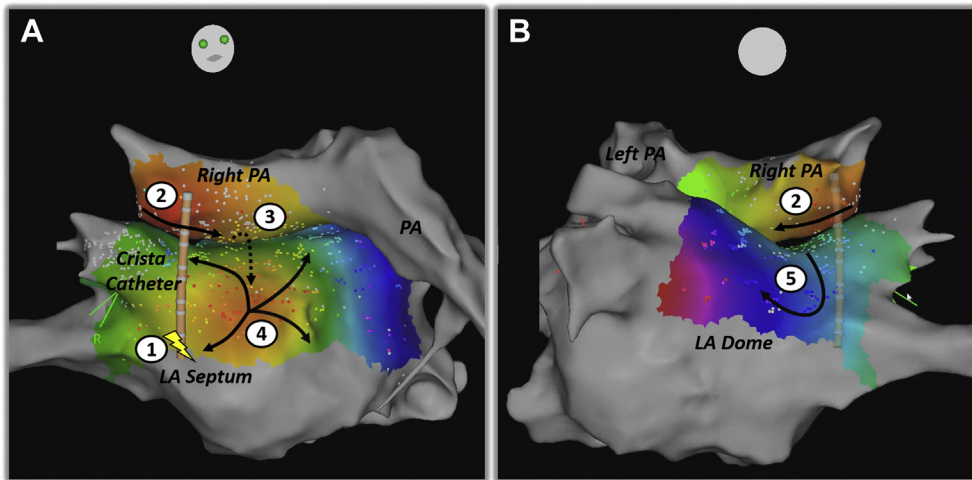


Figure 4 The figure illustrates what we believe to be the first in vivo human recording demonstrating Bachmann bundle (interatrial bundle) right atrium (RA)–to–left atrium (LA) activation (CARTO 3; Biosense Webster, Diamond Bar, CA) with competing epicardial and endocardial wavefronts. **A1:** Pacing from the proximal portion of the crista terminalis catheter at a cycle length of 900 ms. **A2, B2:** Earliest activation recorded in the right pulmonary artery (PA) overlying Bachmann bundle with the wavefront of activation moving away from the septum. **A3:** Epicardial-to-endocardial activation. **A4:** Broad breakthrough pattern of activation on the anterior LA. **B5:** Passive activation of the remaining LA.

other linear LA ablation lines despite demonstrating endocardial entrance and exit block. Complete dissociation of the LA endocardium from the epicardium during AFL has also been reported.⁹ This is explained by the complex bilayer architecture of the LA myocardium.

In a feasibility study of percutaneous epicardial mapping and ablation, Piorkowski and colleagues¹⁰ reported their experience in 59 patients with chronically isolated PV undergoing repeat AF/AFL ablation. In this series, 38% of all endocardial lines required completion by further epicardial ablation to achieve durable block. Similar findings were also reported by Jiang and colleagues.⁹ In their study, 3 out of 16 patients who had PV reconnection continued to have epicardial capture despite endocardial PV reconnection, needing further epicardial ablation. Interestingly, epicardial voltage and activation information could be successfully used to target endocardial ablation sites to achieve posterior wall isolation. In another analysis of the role of epicardial fibers in atypical AFL, Nayak and colleagues²⁵ found evidence of epicardial bridging in almost a third of LA flutters using high-definition mapping. Specifically, epicardial bridges are mediated by the BB for biatrial flutter, ligament of Marshall, and CS for mitral annular flutter and the septopulmonary bundle for roof-dependent atrial flutter.

Catheter ablation of epicardial LA fibers through an endocardial approach is routinely employed in practice but has significant anatomical limitations. Ablation of the LA roof and the ridge between the left PV and the LAA pose specific challenges in this regard. While a percutaneous epicardial approach provides access to a large part of the LA epicardium, catheter manipulation is limited by pericardial reflections that mark the transition from the visceral to parietal pericardium.²⁶ In this regard, mapping and ablation from the epicardial aspect of the LA roof and the LAA ridge from the PA represents a novel approach.

PA–LA anatomy

The PA has a fixed and intimate relationship with the superior aspect of the LA (Figure 6) and is separated from the LA by the transverse sinus.²⁷ After bifurcating, the left PA passes over the left main bronchus and courses parallel to the left superior pulmonary vein (LSPV) with the proximal aspect of the left PA overlying the sulcus between the LSPV and the LAA. In fact, the vestigial fold of the VOM is attached to the inferior surface of the proximal left PA.²⁷ The right PA has a more obtuse takeoff from the bifurcation and courses posterior to the right superior pulmonary vein and the SVC. The proximal aspect of the right PA forms the roof of the transverse sinus and directly overlies the anterosuperior portion of the LA. The PA-to-LA relationship is consistent but the distance appears variable among patients. This space represents multiple components: the PA wall thickness, transverse sinus, epicardial fat, and LA wall thickness. Variability in structure and thickness of these intervening tissues likely accounts for the distance variation between the LA roof and the PA.

Relevance of PA to epicardial bundles

The area of the anterosuperior LA, near the right PA, houses the BB and proximal aspect of the septopulmonary bundle.^{7,28} The BB is composed of thick epicardial layers; runs anterior to the SVC across the septum to the anterior wall of the LA, where it then bifurcates anterior to the LAA; and extends toward the LAA-LSPV ridge.

In sinus rhythm or atrial pacing, mapping of BB from the right PA offers insight into the pathophysiology of this epicardial structure. In patients in whom LA activation occurs primarily over BB, this reflects healthy epicardial conduction and correlates with shorter P-wave durations and interauricular conduction times. The longer P-wave duration and interauricular conduction time in the patient with primary

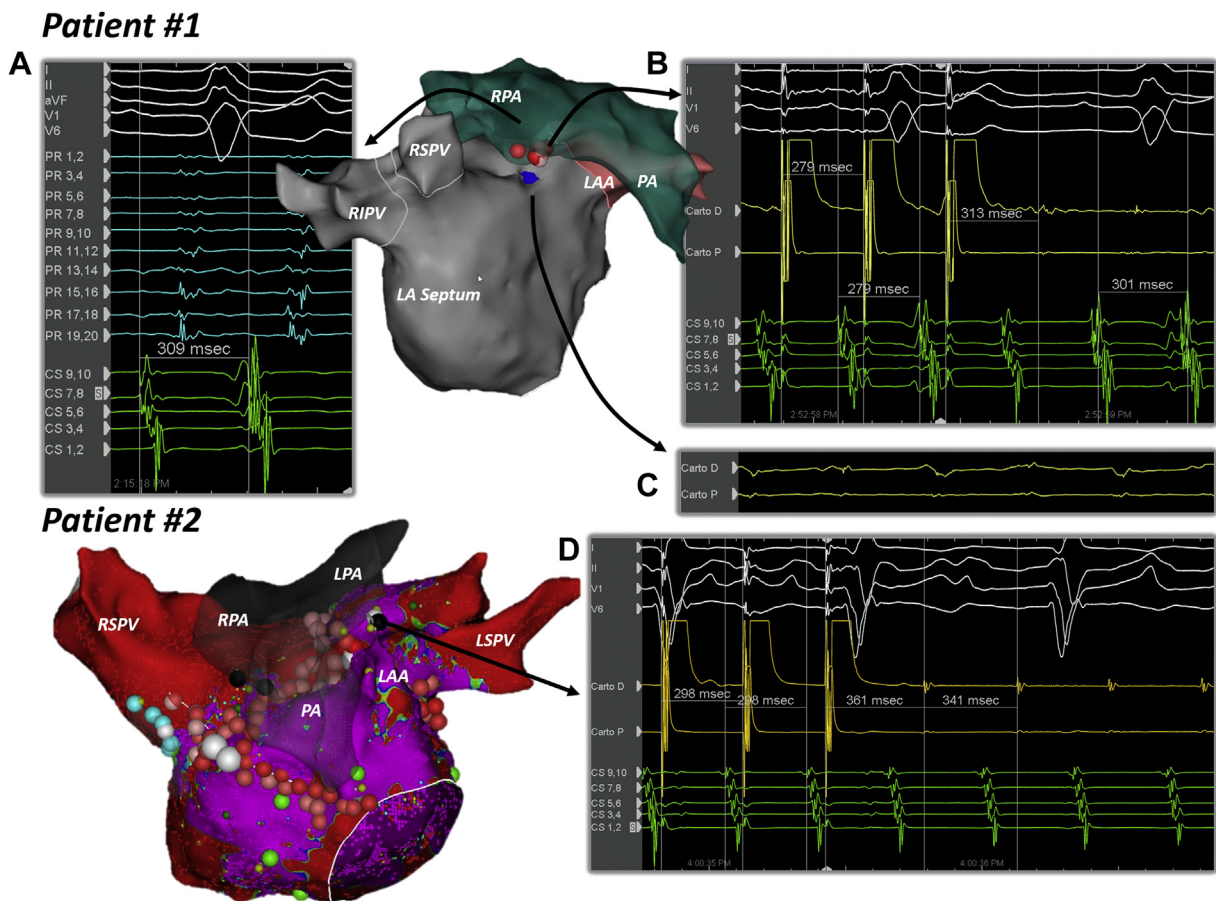


Figure 5 Intracardiac electrograms (EGM) and anatomic maps of atypical atrial flutter (AFL) patient #1 and atypical AFL patient #2. **A:** Patient #1: PentaRay (Biosense Webster, Diamond Bar, CA) in the right pulmonary artery (PA) revealing long continuous signals present during atrial electrical diastole as defined by atrial signals on the coronary sinus catheter. **B:** Patient #1: Entrainment from the ablation catheter in the right PA with a postspacing interval of 12 ms. **C:** Patient #1: Ablation catheter on the adjacent endocardium at the ablation site of termination with a small far-field signal (0.25 mV). Red ball indicates PA ablation lesion; blue ball indicates endocardial ablation termination. **D:** Patient #2: Entrainment from the ablation catheter in the right PA with a postspacing interval of 12 ms. Red ball indicates endocardial ablation lesion, black ball indicates PA ablation lesion. LA = left atrium; LAA = left atrial appendage; LPA = left pulmonary artery; LSPV = left superior pulmonary vein; PA = pulmonary artery; RIPV = right inferior pulmonary vein; RPA = right pulmonary artery; RSPV = right superior pulmonary vein.

septal activation represents delayed propagation over BB bundle and a diseased epicardial state. Mapping the PA will promote further understanding of these epicardial components, elucidate its role in arrhythmogenesis, and reflect the overall health of epicardial/BB conduction.

During right PA pacing, CS activation demonstrated different activation patterns. A possible explanation for this observation could be varying depths of myocardial capture. With distal-to-proximal CS activation, this may reflect sole epicardial capture conducting over BB to the more lateral LA compared with both endocardial and epicardial capture, representing a more physiologic activation process with proximal-to-distal CS activation. Alternatively, this could simply reflect more proximal or distal right PA pacing and capture, correlating with more septal or lateral atrial myocardial capture. Lastly, these different patterns could also occur secondary to prior ablation and reflect delay or block in this region. This was not the case in our present study, as none of the patients with CS activation recordings had prior LA roof or LA dome ablation.

Regarding atypical AFL, an anterior mitral line connecting the mitral annulus to the right superior pulmonary vein runs through the BB region and poses a challenge to successful transmural ablation. Even when endocardial block across the line is achieved, there is preserved epicardial conduction across this region, which can then form a substrate for developing biatrial flutter. Mapping of this region from the right PA can assist with designing ablation lines, like using epicardial posterior wall activation and signals to guide anatomical endocardial ablation.²⁹ In our first atypical flutter case, we were able to use the recordings from the PA to select an optimal endocardial ablation site in the LA roof with successful flutter termination. Similar relationships of the right PA to the proximal septopulmonary bundle make it relevant while targeting roof-dependent flutters as well as interrupting epicardial connections to the LA posterior wall, as demonstrated in 1 of our atypical flutter patients. The left PA can be used to record epicardial signals from the LAA ridge and can potentially serve as a vantage point for recording and optimizing targeted ablation, with either epicardial

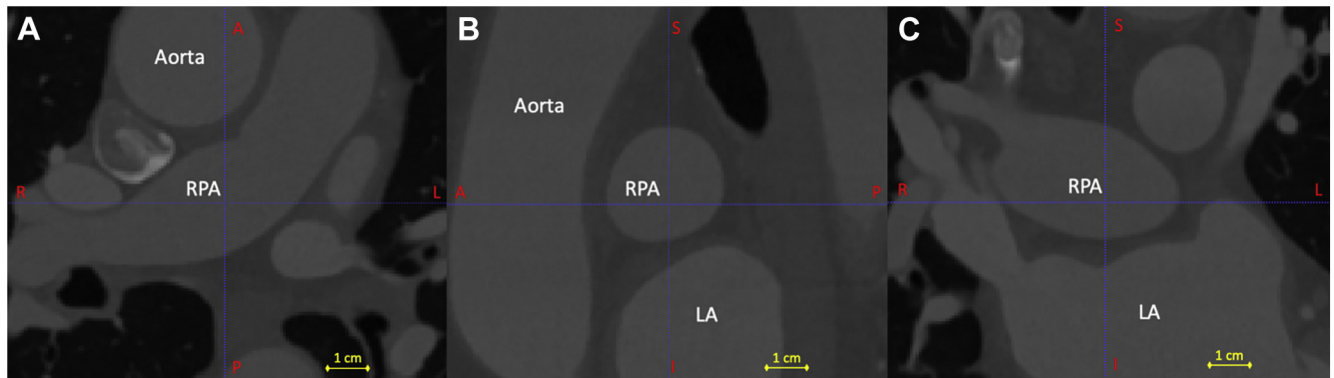


Figure 6 Contrast-enhanced computed tomography image showing the anatomical relationship of the pulmonary artery to the left atrium (LA). **A:** Axial plane showing the right pulmonary artery (RPA) as it courses posterior and rightward behind the aorta. **B:** Sagittal plane showing the RPA directly overlying the LA roof. **C:** Coronal plane showing the RPA directly overlying the LA roof.

radiofrequency ablation or VOM ethanol infusion, to augment an endocardial lateral mitral line.

Ablation within the PA

Delivering radiofrequency energy within venous structures such as the CS is commonly performed. Biophysics of energy delivery are limited by thin vessel walls, high impedance, and inadequate power delivery because of a “heat sink” caused by blood flow in the coronary venous system. While ablation within the aortic and pulmonic cusps is performed for ventricular arrhythmias, the tissue targeted for ablation is smooth muscle sleeves that extend over the vasculature. Effects of ablation in arterial structures beyond the semilunar valves without intervening muscle are unknown. Ablation from the PA had dynamic effects in 2 of 3 cases and swine ablation revealed lesion penetration to the epicardial LA. Optimal ablation settings for safety and efficacy are not known and anatomic variability in distance may play a critical role. Perhaps threshold of myocardial capture will guide future ablation from the PA as a surrogate for proximity and an index of direct continuity.³⁰ Concerns include increased risk of pericardial or pleural effusion with catheter manipulation to the distal PA and branches, injury to nearby structures such as the sinus node artery, ablation of BB with RA-to-LA uncoupling, PA-to-LA fistula formation, or disruption of the PA itself.³¹ Ablation from the PA, in unipolar or bipolar mode, warrants further study before it is routinely performed in this region.

Limitations

The generalizability of this study is limited by the small sample size and our present investigation represents a feasibility and proof-of-concept study. There was variability in the PA mapping catheter based on provider preference, either a multipolar catheter or an ablation catheter. In addition, variability in the patient’s rhythm during PA mapping may also affect signal amplitudes. The PA-to-endocardial LA distance is variable and the accuracy of the mapping system distance tool likely only provides an estimated distance, given the

anatomical distortion that can occur during electroanatomic mapping. Formal imaging with computerized tomography or magnetic resonance imaging will provide more accurate measurements. Attempts at LA capture from the PA were performed with binary standard and high-output pacing and true capture thresholds were not determined.

Conclusion

Natural surface epicardial mapping from the right and left main PA is a means for electrogram recording of BB and epicardial roof muscle fibers. Epicardial signals from the PA can be safely recorded and in select cases of atypical flutter, the arrhythmia can be successfully entrained from this location. These observations provide arrhythmia characteristics that may not be otherwise visible on the LA endocardial surface. The safety and efficacy of an adjunctive strategy of unipolar ablation from the PA, or bipolar ablation using an electrode at the PA and the other at the opposing endocardial LA, requires further study.

Funding Sources

This work was supported by the Mark Marchlinski EP Research and Education Fund and indirectly by NIH R01HL142893 awarded to Dr Nazarian.

Disclosures

Dr Nazarian receives research funding from the United States NIH/NHLBI, ImriCor, Biosense Webster, and ADAS Software. He has also received consultant and speaker fees from Circle Software, Biosense Webster, ImriCor, and CardioSolv. The University of Pennsylvania Conflict of Interest Committee manages all commercial arrangements. The other authors declare no conflicts of interest.

Authorship

All authors attest they meet the current ICMJE criteria for authorship.

Patient Consent

All patients gave informed consent for the use of clinical, imaging, and procedural data for medical research prior to the procedure.

Ethics Statement

Clinical Studies: The Institutional Review Board of the Hospital of the University of Pennsylvania approved our prospective Atrial Fibrillation Registry Cohort.

Animal Experiments: The research protocol was approved by the Institutional Animal Care and Use Committee of the University of Pennsylvania and conformed to the position of the American Heart Association on Research Animal Use.

Disclaimer

Given his role as Section Editor, Saman Nazarian had no involvement in the peer review of this article and has no access to information regarding its peer review. Full responsibility for the editorial process for this article was delegated to Editors Nazem Akoum and Jeanne E. Poole.

Appendix

Supplementary data

Supplementary data associated with this article can be found in the online version at <https://doi.org/10.1016/j.hroo.2021.10.003>.

References

- Bachmann G. The inter-auricular time interval. *American Journal of Physiology* 1916;41:309–320.
- James TN. The connecting pathways between the sinus node and a-v node and between the right and the left atrium in the human heart. *Am Heart J* 1963; 66:498–508.
- Khaja A, Flaker G. Bachmann's bundle: does it play a role in atrial fibrillation? *Pacing Clin Electrophysiol* 2005;28:855–863.
- Teuwen CP, Does L, Kik C, et al. Sinus rhythm conduction properties across Bachmann's bundle: impact of underlying heart disease and atrial fibrillation. *J Clin Med* 2020;9.
- Teuwen CP, Yaksh A, Lanter EA, et al. Relevance of conduction disorders in Bachmann's bundle during sinus rhythm in humans. *Circ Arrhythm Electrophysiol* 2016;9:e003972.
- Glover BM, Hong KL, Baranchuk A, Bakker D, Chacko S, Bisleri G. Preserved left atrial epicardial conduction in regions of endocardial "isolation." *JACC Clin Electrophysiol* 2018;4:557–558.
- Garcia F, Enriquez A, Arroyo A, Supple G, Marchlinski F, Saenz L. Roof-dependent atrial flutter with an epicardial component: role of the septopulmonary bundle. *J Cardiovasc Electrophysiol* 2019;30:1159–1163.
- Yorgun H, Sezenoz B, Aytemir K. Epicardial ablation of recurrent left atrial macroreentrant tachycardia from Bachmann's bundle region after endocardial ablation. *Pacing Clin Electrophysiol* 2021;44:1474–1476.
- Jiang R, Buch E, Gima J, et al. Feasibility of percutaneous epicardial mapping and ablation for refractory atrial fibrillation: insights into substrate and lesion transmural. *Heart Rhythm* 2019;16:1151–1159.
- Piorkowski C, Kronborg M, Houdain J, et al. Endo-/epicardial catheter ablation of atrial fibrillation: feasibility, outcome, and insights into arrhythmia mechanisms. *Circ Arrhythm Electrophysiol* 2018;11:e005748.
- Tahir K, Kiser A, Caranasos T, Mounsey JP, Gehi A. Hybrid epicardial-endocardial approach to atrial fibrillation ablation. *Curr Treat Options Cardiovasc Med* 2018; 20:25.
- Rao S, Kwasnik A, Tung R. Direct epicardial recordings in the region of the septopulmonary bundle: anatomy "behind" posterior wall activation. *JACC Clin Electrophysiol* 2020;6:1214–1216.
- Chaffanjon P, Brichon PY, Faure C, Favre JJ. Pericardial reflection around the venous aspect of the heart. *Surg Radiol Anat* 1997;19:17–21.
- Hwang C, Chen PS. Ligament of Marshall: why it is important for atrial fibrillation ablation. *Heart Rhythm* 2009;6:S35–S40.
- Boyle NG, Shivkumar K. Epicardial interventions in electrophysiology. *Circulation* 2012;126:1752–1769.
- Daher R, Chouillard E, Panis Y. New trends in colorectal surgery: single port and natural orifice techniques. *World J Gastroenterol* 2014;20:18104–18120.
- Voermans RP, Van Berge Henegouwen MI, Fockens P. Natural orifice transluminal endoscopic surgery (notes). *Endoscopy* 2007;39:1013–1017.
- January CT, Wann LS, Alpert JS, et al. 2014 AHA/ACC/HRS guideline for the management of patients with atrial fibrillation: a report of the American College of Cardiology/American Heart Association task force on practice guidelines and the heart rhythm society. *Circulation* 2014;130:e199–e267.
- Ogawa S, Dreifus LS, Kitchen JG 3rd, Shenoy PN, Osmick MJ. Catheter recording of Bachmann's bundle activation from the right pulmonary artery: a new technique for atrial mapping and the study of supraventricular tachycardia. *Am J Cardiol* 1978;41:1089–1096.
- Leier CV, Jewell GM, Magorien RD, Wepsic RA, Schaal SF. Interatrial conduction (activation) times. *Am J Cardiol* 1979;44:442–446.
- Kobza R, Hindricks G, Tanner H, et al. Late recurrent arrhythmias after ablation of atrial fibrillation: incidence, mechanisms, and treatment. *Heart Rhythm* 2004; 1:676–683.
- van Campenhout MJ, Yaksh A, Kik C, et al. Bachmann's bundle: a key player in the development of atrial fibrillation? *Circ Arrhythm Electrophysiol* 2013; 6:1041–1046.
- Barrio-Lopez MT, Sanchez-Quintana D, Garcia-Martinez J, et al. Epicardial connections involving pulmonary veins: the prevalence, predictors, and implications for ablation outcome. *Circ Arrhythm Electrophysiol* 2020;13:e007544.
- Tung R. Percutaneous epicardial ablation of atrial fibrillation. *Card Electrophysiol Clin* 2020;12:371–381.
- Nayak HM, Aziz ZA, Kwasnik A, et al. Indirect and direct evidence for 3-d activation during left atrial flutter: anatomy of epicardial bridging. *JACC Clin Electrophysiol* 2020;6:1812–1823.
- Pak HN, Hwang C, Lim HE, Kim JS, Kim YH. Hybrid epicardial and endocardial ablation of persistent or permanent atrial fibrillation: a new approach for difficult cases. *J Cardiovasc Electrophysiol* 2007;18:917–923.
- McAlpine WA, Springer V. Heart and Coronary Arteries: An Anatomical Atlas for Clinical Diagnosis, Radiological Investigation, and Surgical Treatment. Berlin; New York: Springer-Verlag; 1975.
- Pambrun T, Duchateau J, Delgove A, et al. Epicardial course of the septopulmonary bundle: anatomical considerations and clinical implications for roof line completion. *Heart Rhythm* 2021;18:349–357.
- Smietana JJ, Pothineni NVK, Nazarian S. Thinking outside the box: epicardial mapping of atypical flutter. *JACC Clin Electrophysiol* 2021;7:825–827.
- Squara F, Desjardins B, Marchlinski FE, Supple GE. Prospective 3-dimensional computed tomography segmentation of the pericardiac right phrenic nerve in the setting of atrial fibrillation ablation. *Circ Arrhythm Electrophysiol* 2014;7:561–562.
- Pardo Meo J, Scanavacca M, Sosa E, et al. Atrial coronary arteries in areas involved in atrial fibrillation catheter ablation. *Circ Arrhythm Electrophysiol* 2010;3:600–605.